Electric Power Systems Research 219 (2023) 109242

Contents lists available at ScienceDirect

Electric Power Systems Research

journal homepage: www.elsevier.com/locate/epsr

Size/location estimation for loss of generation events in power systems with high penetration of renewables

Jesús Sánchez Cortés [a,*], Mohammad Rezaei Jegarluei [a], Petros Aristidou [b], Kang Li [a], Sadegh Azizi [a]

[a] School of Electronic and Electrical Engineering, University of Leeds, Leeds, LS2 9JT, United Kingdom
[b] Department of Electrical Engineering, Computer Engineering and Informatics, Cyprus University of Technology, Limassol, 3026, Cyprus

ARTICLE INFO

Keywords:
Loss of generation
Renewable energy sources
Synchrophasor
Superimposed circuit
Sum of squared residuals

ABSTRACT

The increasing penetration of renewable energy sources (RESs) is significantly impacting the performance of traditional control and protection schemes employed in power systems. The early detection and size estimation of loss of generation (LoG) events contribute to the timely provision of remedial actions required to preserve the frequency stability of the system. This paper proposes an effective method for locating and estimating the size of LoG events in power systems with high penetration of RESs. A system of linear equations for every candidate LoG location is formulated based upon KVL and KCL equations. Suitable nodal current sources are employed to model RESs and the candidate tripped generator in the superimposed circuit. The nodal current injections of RESs are estimated based on their power setpoints and available measurements provided by PMUs. The solution of the systems of equations established provides the LoG location and size using the least-squares method. The proposed method is more accurate than existing LoG identification methods that resort to frequency measurements and the knowledge of system inertia. Centralized under-frequency load shedding is presented as a potential application for the proposed method. Extensive simulations conducted on the IEEE 39-bus test system verify the effectiveness and accuracy of the proposed method.

1. Introduction

Renewable energy sources (RESs) are progressively integrated into power systems globally as a result of significant efforts to meet the carbon reduction targets imposed by environmental policies concerning climate change [1,2]. RESs are intermittent in nature and are connected to the power system via power electronics interfaces, thereby providing little or no inertia to the system [3]. This makes the inertia of the power system volatile with a highly reduced lower boundary [4]. This is seen as a pressing challenge for modern power systems, as inertia relates to the power system's stiffness against frequency deviations caused by loss of generation (LoG) events [5–7].

Frequency nadir, which is the lowest frequency reached following an event, depends on how fast the remedial action is adopted to arrest the frequency decline. LoG events may lead to excessively low-frequency nadirs if the active power mismatch is not compensated promptly enough. This might trigger cascading trips of other generating units [8], thus jeopardizing system stability.

Under-frequency load shedding (UFLS) is a well-established remedial action against large LoG events [5]. The key aim of UFLS is to recover the active power balance by disconnecting an appropriate amount of load from the power system. In conventional UFLS schemes, a certain amount of load is shed if the local frequency falls below a pre-specified threshold on its decaying trajectory after an LoG event [8]. Conventional UFLS is inherently slow, and thus, some adaptive UFLS schemes have been introduced over the past two decades to expedite the load shedding process. Relying upon the swing equation of the center of inertia, these methods assume relatively constant inertia for the system to estimate the size of LoG events [9]. In power systems with high penetration of renewables, however, inertia is highly volatile. This makes the underlying assumptions of adaptive methods invalid [3]. For instance, a high rate of change of frequency (RoCoF) does not necessarily indicate a large LoG size. As a result, these methods might fail to prevent extremely low nadirs or may lead to over-shedding [10].

Most methods for locating and estimating the size of LoG events are based on frequency measurements. The assumption of [7] and [11] is

* Corresponding author.
E-mail address: eljsc@leeds.ac.uk (J. Sánchez Cortés).

https://doi.org/10.1016/j.epsr.2023.109242
Received 24 October 2022; Received in revised form 31 January 2023; Accepted 21 February 2023
Available online 1 March 2023

the availability of specific sets of frequency measurements to estimate the LoG size at any location. The recorded dynamic data of past events obtained from frequency disturbance recorders (FDRs) are compared to frequency deviations to approximate the size of LoG events in [12–14]. In [7], the frequency propagation speed (FPS) is employed to calculate the electrical distance between the LoG location and the FDRs. References [15] and [16] incorporate a trigger algorithm based on the RoCoF for identifying LoG events. These methods assume the frequencies of all generating units are reliably collected at the control center, which is not always possible [17]. Furthermore, due to the measurement noise and the variation in the rotational speed of the remaining generation, RoCoF calculation loses accuracy for a couple of hundreds of milliseconds after the LoG event [18]. Therefore, there is an unavoidable time delay between the LoG event and a reliable RoCoF measurement [18,19].

Another promising research avenue is using phasor measurement units (PMUs) to monitor frequency variations in real-time at different locations in the power system. In [20] and [21], the disturbance arrival time is utilized to estimate the FPS of LoG events, and then the location and size of the tripped generator are calculated. The complexity in the electrical distance calculation compromises the accuracy of the LoG localization by this approach. On the other hand, [22] and [23] use the aggregate inertia and the swing equation to detect the LoG event and estimate its size. In these methods, however, all generator frequencies should be monitored. This requirement contradicts the purpose because having measurements and communication infrastructure at all generating units would enable direct identification of the tripped generation using its circuit breaker status. To avoid using frequency measurements, [24] detects significant changes in the generation through active power measurements by relying on the SCADA/EMS. These methods are computationally expensive and can provide accurate results only if a fixed set of measurements is available.

Reference [25] uses the impedance matrix with sparse PMU measurements to identify the change in the nodal current injection at the LoG location. The application of voltage and current data taken from one or two cycles following the event makes the method faster than those using frequency measurements. This method, however, does not account for RESs, which introduces inaccuracies in modeling the system, thus reducing its accuracy in systems with high penetration of renewables.

This paper presents a method for locating and estimating the size of LoG events in power systems with high penetration of RESs. First, the candidate tripped generation is replaced by a nodal current source in the superimposed circuit, as is every RES with PMU measurements in the system initially. Next, the nodal current injection of each RES without PMU measurements is calculated based on its active and reactive power setpoints and terminal voltage. Finally, an index is obtained using the ordinary least squares (OLS) method to locate the actual tripped generation. The proposed method can function with any two independent synchrophasors and places no rigid constraint on the location or the number of PMUs. The method does not require frequency measurements, nor does it rely on the knowledge of system inertia.

The remainder of this paper is organized as follows. Section 2 describes the superimposed circuit methodology for determining the location and size of LoG events. The modeling technique proposed to account for RESs in the superimposed circuit is detailed in Section 3. Extensive simulations are discussed in Section 4. Section 5 puts forward the conclusions drawn from this research work.

As discussed in [26] and [27], an effective wide-area generation outage monitoring method must be able to reliably identify the size and location of LoG events in a short period of time. Research gaps that need to be addressed are practical challenges such as partial coverage of PMUs, communication latencies, and different numbers and penetration levels of RESs [27]. Existing approaches that utilize frequency/RoCoF measurements cannot provide fast and accurate results as these measurements are not reliable for a few hundred milliseconds following the LoG inception [18]. Furthermore, approaches that rely upon the swing equation assume relatively constant inertia for the power system, whilst this variable becomes highly volatile in systems with high penetration levels of RESs [3]. To address these challenges, the formulation set forth is based on the Substitution Theorem in Circuit Theory to enable the modeling of RESs as unknown current sources with no underlying assumptions. The resulting algebraic equations, along with the fact that the sum of squared residuals for a pertinent system of equations must be zero, make it possible to identify both the location and size of LoG events. This is achieved in a short period of time without resorting to differential swing equations. In this context, the salient features of the proposed method and its advantages over existing ones can be summarized as follows:

- Addressing the presence of RESs regardless of their penetration level and locations
- Fast decision-making thanks to the independence from frequency/RoCoF measurements
- Accurate estimation of LoG location and size
- Placing no rigid limitations on the PMU number and locations
- Robustness against measurement and parameter errors

2. Identification of LoG events

In this section, the formulation for determining the size and location of LoG events in the presence of RESs is put forward. This will be based on the superimposed circuit methodology and requires data routinely available to the control center, such as the bus impedance matrix of the power system, PMU data, and active and reactive power setpoints of the RESs as input. A system of linear equations is derived for every candidate LoG location and is then solved using the OLS method. The minimum sum of squared residuals (*SoSR*) resulting from the solution of these systems of equations is used to locate the LoG event.

The superimposed circuit methodology essentially concerns disturbances on nodal injections of a circuit with a fixed bus impedance matrix. To be able to apply it, the lost generation is entirely replaced by an unknown current source, as shown in Fig. 1. This is regardless of whether the lost generation is a synchronous generator (SG), an RES, or a combination of both. All other SGs can be safely replaced by their subtransient impedances in the superimposed circuit within the time frame of interest to this study [28]. The RESs, however, cannot be simply modeled by constant impedances. This is because the equivalent impedance of an RES is not predetermined and depends on many factors. These include pre-LoG voltage and current phasors, which might not be available if there is no PMU at the RES terminal [29]. Therefore, RESs are also replaced by unknown current sources in the superimposed circuit, as depicted in Fig. 1.

2.1. System of equations for each candidate LoG location

Let us consider an LoG event at bus k. The superimposed voltage measured by a PMU at any other bus in the system, e.g., bus w, denoted by ΔV_w^m, satisfies the equation below in each sequence circuit:

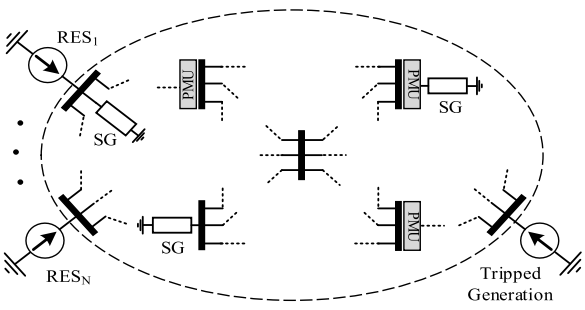

Fig. 1. Superimposed circuit corresponding to an LoG event.

$$\Delta V_w^m = \sum_{r=1}^{N} Z_{w,r}\Delta I_r^{RES} + Z_{w,k}\Delta I_k + e_w \tag{1}$$

where the superscript "m" refers to measured quantities and e_w represents the measurement error. $Z_{w,r}$ is the (w,r)-th entry of the bus impedance matrix, and ΔI_r^{RES} is the superimposed nodal current of the RES at bus r. Besides, ΔI_k denotes the superimposed nodal current of the tripped generation at bus k, and 1 to N are the indices of the buses to which RESs are connected.

The measured superimposed current of the sending-end of the transmission line u- w in each sequence circuit, denoted by ΔJ_{uw}^m, can be written as a function of the superimposed currents as below:

$$\Delta J_{uw}^m = \sum_{r=1}^{N} C_{uw,r}\Delta I_r^{RES} + C_{uw,k}\Delta I_k + e_{uw} \tag{2}$$

where $C_{uw,k}$ is the current transfer coefficient whose derivation is detailed in [28], and e_{uw} is the measurement error. Provided that ΔI_r^{RES} is directly measured by a PMU, the equation below can be established for this measurement:

$$\Delta I_r^{m,RES} = \Delta I_r^{RES} + e_r \tag{3}$$

Let p denote the number of available synchrophasors provided by PMUs and N be the number of RESs in the power system. For each candidate LoG location, denoted by c, a system of linear equations can be formed in each sequence circuit for the p measurements using their corresponding equations of type (1), (2), or (3) as follows:

$$\boldsymbol{m}_{p\times 1} = \boldsymbol{H}^c{}_{p\times(1+N)}\boldsymbol{x}^c{}_{(1+N)\times 1} + \boldsymbol{e}_{p\times 1} \tag{4}$$

where $\boldsymbol{m}$, $\boldsymbol{H}^c$, and $\boldsymbol{e}$ are the superimposed measurements vector, coefficient matrix corresponding to the location c, and error vector, respectively. The vector of unknowns, denoted by $\boldsymbol{x}^c$, contains the superimposed current injections of the candidate tripped generation and all RESs as:

$$\boldsymbol{x}^c = \begin{bmatrix} \Delta I_c & \Delta I_1^{RES} & \cdots & \Delta I_N^{RES} \end{bmatrix}^T \tag{5}$$

The system of equations (4) can be solved using the OLS method as follows:

$$\widehat{\boldsymbol{x}}^c = \left(\boldsymbol{H}^{c^*}\boldsymbol{H}^c\right)^{-1}\boldsymbol{H}^{c^*}\boldsymbol{m} \tag{6}$$

where $(\cdot)^*$ denotes the conjugate transpose. The vector $\widehat{\boldsymbol{x}}^c$ contains the estimated unknowns corresponding to the location c.

2.2. LoG location and size estimation

Identifying the LoG location could be advantageous in preserving the power system's voltage and frequency stabilities. As detailed in [30], the power system's stability can sometimes be preserved only by conducting load shedding in the vicinity of the LoG event. In this subsection, the proposed method for estimating the location and size of LoG events is put forward.

As LoGs are symmetrical events, the system of equations (4) is built for the positive-sequence circuit for every candidate LoG location. The objective function of the OLS method is to minimize the *SoSR*. If the measurements were error-free, the *SoSR* would be zero for the tripped generation since all equations in (4) hold true with respect to the measurements. In practice, however, the *SoSR* of the tripped generation might be slightly greater than zero due to measurement errors and topology changes [28]. On the contrary, the *SoSR* of other candidates will take non-negligible values as their coefficient matrix does not correspond to the true LoG location. Thus, in this paper, the candidate LoG location with the smallest *SoSR* is identified as the true LoG location as follows:

$$k = Arg\left\{\min_{\forall c\in\boldsymbol{G}} SoSR_c = [\boldsymbol{m} - \boldsymbol{H}^c\widehat{\boldsymbol{x}}^c]^*[\boldsymbol{m} - \boldsymbol{H}^c\widehat{\boldsymbol{x}}^c]\right\} \tag{7}$$

where $\boldsymbol{G}$ is the set of all candidate LoG locations. Once the LoG event has been located, the superimposed current of the tripped generation estimated by (6) can be used to estimate the LoG size. The change in the complex power generation at the LoG location, i.e., ΔS_k, can be obtained from:

$$\Delta S_k = (V_k^{pre} + \Delta V_k)(I_k^{pre} + \Delta I_k)^* - V_k^{pre} I_k^{pre*} \tag{8}$$

Eq. (8) can be written as:

$$\Delta S_k = V_k^{pre}\Delta I_k{}^* + \Delta V_k \left(|I_k^{pre}|e^{-j\varphi} + \Delta I_k{}^* \right) \tag{9}$$

where V_k^{pre} is the pre-LoG voltage at bus k, which is assumed to be known in the control center through state estimation using existing SCADA and PMU measurements [31]. $|I_k^{pre}|$ and φ denote the pre-LoG current injection magnitude and power angle at bus k, respectively, which are assumed to be known upon the outage.

2.3. Discrimination between faults and LoG events

As explained, the tripped generation is modeled by a nodal current injection at the generation bus. However, a short-circuit fault occurring at that bus can also be represented by a nodal current injection in the same way as was done for the LoG event. Thus, following a short-circuit fault at a generation bus, the minimum *SoSR* calculated by (7) will refer to that bus. Therefore, some criteria are needed to differentiate between a fault and an LoG event at a generation bus.

Considering that LoG events only contain positive-sequence components, the presence of considerable negative-sequence quantities in the measurements readily indicates an asymmetrical short-circuit fault in the system. On the other hand, in the case of symmetrical faults at a generation bus, it can be demonstrated that the magnitude of the superimposed nodal current at that bus will always be higher than that of the pre-LoG current injection, i.e., $|I_k^{pre}|$. However, the superimposed nodal current representing an LoG event will always be equal to or less than the pre-LoG current injection. These simple criteria can easily be employed for discriminating faults from LoG events at generation buses.

3. Accounting for the presence of RESs

The measured superimposed nodal currents of monitored RESs, i.e., RESs with a PMU at their terminals, can readily be incorporated into the equations of type (4) using (3). The inclusion of such measured $\Delta I_r^{m,RES}$ in the unknown vector does not create any solvability concerns [32]. This is because every row in the coefficient matrix corresponding to a monitored RES has only one entry equal to one, while all other entries in that row are zeros. The inclusion of such a row in the coefficient matrix will increase its rank by one [32].

The solution of the system of linear equations (4) provides an estimation for the superimposed nodal currents of the candidate tripped generation and all non-monitored RESs (RESs without a PMU at their terminals). However, if the penetration level of RESs is high, the number of unknowns might exceed the number of dependent equations in (4), which could make the system unsolvable.

To avoid solvability concerns, the superimposed nodal currents of non-monitored RESs are initially ignored from the unknown vector $\boldsymbol{x}^c$. This is to obtain an initial estimation for the superimposed nodal current at each candidate location. This also provides an initial estimate for the superimposed voltages at the terminals of non-monitored RESs based on (1). Next, the unknown superimposed current injections of non-monitored RESs can be estimated and included in the corresponding equations. This helps to update the value of the superimposed nodal current representing the candidate tripped generation. This process is

continued until the changes resulting from an iteration are negligible, i.e., the changes made in all estimated superimposed nodal current injections are below a pre-specified tolerance of 1×10^{-4}. Finally, the corresponding *SoSR* for each candidate location is calculated to determine the true LoG location. The whole procedure is detailed in the following subsections.

3.1. Initial estimations ignoring non-monitored RESs

As described in Section 2, every RES is replaced by a suitable current source in the superimposed circuit. The superimposed nodal current of the RES can be directly measured when the RES terminal is equipped with a PMU. However, it may not be possible to have PMUs at certain substations due to budget/infrastructure constraints. Even if all RESs terminals had PMUs, it would not be rational to assume all PMU data are received in time due to the unpredictability of communication latency and the possibility of data losses.

Disregarding the superimposed nodal currents of the non-monitored RESs, the system of equations (4) is reformed as:

$$\boldsymbol{m}_{p\times 1} = \boldsymbol{H}^{c}_{p\times(1+q)}\boldsymbol{x}^{c}_{(1+q)\times 1} + \boldsymbol{e}_{p\times 1} \tag{10}$$

where the matrix $\boldsymbol{H}^{c}$ contains the coefficients related to the candidate LoG location and the monitored RESs. The vector $\boldsymbol{x}^{c}$ is composed of the superimposed nodal current at the candidate location, i.e., ΔI_c, and those of the monitored RESs, respectively. The index q denotes the number of monitored RESs. The system of equations (10) can easily be solved using the OLS method as follows:

$$\widehat{\boldsymbol{x}}^{c} = \left(\boldsymbol{H}^{c^*}\boldsymbol{H}^{c}\right)^{-1}\boldsymbol{H}^{c^*}\boldsymbol{m} \tag{11}$$

where $\widehat{\boldsymbol{x}}^{c}$ contains the initial estimation of the superimposed nodal current representing the candidate tripped generation and the monitored RESs. Eq. (10) is solved for every candidate location. Then, using the initial estimation of $\widehat{\Delta I}_c$ and the superimposed currents of the monitored RESs, an initial estimation for the superimposed voltage at all buses can be obtained from (1). The superimposed nodal current at the candidate location is updated after incorporating the non-monitored RESs into the formulation, as explained in the following subsection.

3.2. Modeling non-monitored RESs

In this subsection, a method is presented to approximate the superimposed nodal currents of the non-monitored RESs. This is accomplished using the pre-LoG active and reactive power of RESs and the estimated superimposed voltages at their terminals. Our assumption in this study is that LoG events do not lead any RES into the low-voltage ride-through operation mode. This means the terminal voltage of none of the RESs drops more than 10% following an LoG event, which is in accordance with the N-1 security criterion. Hence, non-tripped RESs hold the active and reactive power injections equal to the pre-set references according to the relevant grid codes [33,34].

Let us consider a non-monitored RES connected to bus r. The currents injected by this RES before and after the LoG event can be expressed as follows:

$$I_r^{pre} = \frac{\left(P_{ref} - jQ_{ref}\right)}{\left(V_r^{pre}\right)^*} \tag{12}$$

$$I_r^{post} = \frac{\left(P_{ref} - jQ_{ref}\right)}{\left(V_r^{post}\right)^*} \tag{13}$$

where I_r^{pre} is the pre-LoG current injection of the RES and P_{ref} and Q_{ref} are the pre-LoG active and reactive power references of the RES. The superscript "*post*" is used to refer to the post-LoG values. V_r^{post} is calculated using V_r^{pre} and ΔV_r, which are the pre-LoG and superimposed voltages at the RES terminal. The superimposed current of the non-monitored RES can be obtained by subtracting (12) from (13) as below:

$$\Delta I_r^{n,RES} = \left(P_{ref} - jQ_{ref}\right)\left(\frac{1}{V_r^{pre} + \Delta V_r} - \frac{1}{V_r^{pre}}\right)^* \tag{14}$$

Now, the superimposed nodal currents of non-monitored RESs are included in the vector $\boldsymbol{m}$ in (4) as virtual measurements. Accordingly, the rows related to such superimposed currents are added to the coefficient matrix. As explained, including such a row in the coefficient matrix will increase its rank by one. This eliminates the concerns over the solvability of (4) and enables updating the estimation of $\widehat{\Delta I}_c$ by solving (6) for every candidate location.

3.3. Algorithm for implementation of the proposed method

The superimposed nodal currents of the tripped generation and non-monitored RESs are estimated and updated through an iterative algorithm to improve the accuracy of the modified set of equations. The flowchart shown in Fig. 2 can be used for the near real-time implementation of the proposed method. The algorithm represented by this flowchart to identify the LoG location and size is detailed below:

(i) All non-monitored RESs are first excluded from the superimposed circuit. This gives rise to (10), eliminating the concerns over the solvability of (4).
(ii) The solution of (10) using (11) provides a starting point for the estimation of the superimposed nodal current at the candidate location, i.e., $\widehat{\Delta I}_c$.
(iii) The superimposed voltages at the terminals of non-monitored RESs are obtained from (1). In the first iteration, the $\widehat{\Delta I}_c$ used for this calculation is taken from step (ii). In the next iterations, $\widehat{\Delta I}_c$ estimated in step (v) of the previous iteration will be utilized.
(iv) The superimposed nodal currents of non-monitored RESs, $\Delta I_r^{n,RES}$, are computed using (14). These currents are included in the measurements vector in (4) as virtual measurements. Accordingly, the rows representing the equations of type (3) for such virtual

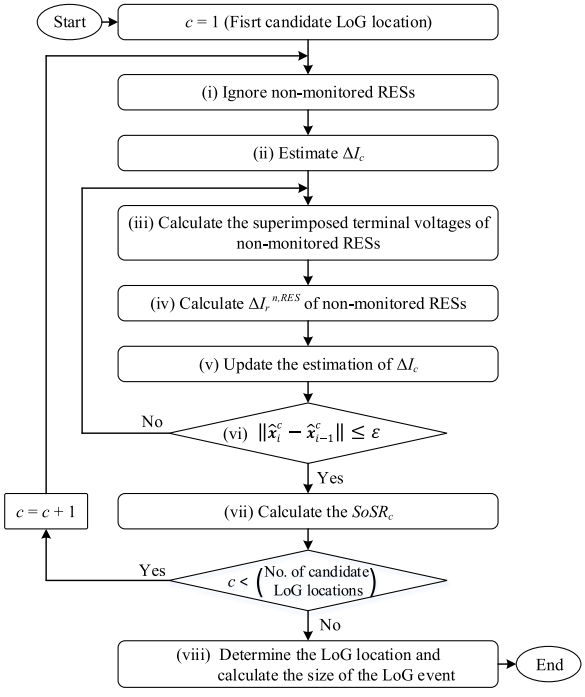

Fig. 2. Flowchart of the proposed method.

measurements are added to the coefficient matrix. The superimposed nodal currents of monitored RESs, $\Delta I_r^{m,RES}$, are provided by the corresponding PMU measurement.

(v) The resulting set of equations is solved by (6) for the candidate LoG location to update $\widehat{\Delta I}_c$. This calculation accounts for the superimposed nodal currents of all monitored and non-monitored RESs.

(vi) The algorithm goes back to step (iii) to update the superimposed voltages and currents of non-monitored RESs through another iteration. To terminate the process, the most recent estimation of the vector of unknowns, i.e., $\widehat{x}_i^c$ including all $\Delta I_r^{m,RES}$ and $\widehat{\Delta I}_c$, are compared to that of the previous one, i.e., $\widehat{x}_{i-1}^c$. If the norm of the difference between $\widehat{x}_i^c$ and $\widehat{x}_{i-1}^c$ is less than the specified tolerance, ε, the iteration is terminated and the algorithm goes to step (vii).

(vii) The *SoSR* of the candidate LoG location is computed. Steps (ii) to (vii) are conducted for every candidate location.

(viii) The LoG location is determined using (7). Finally, the amounts of the lost active and reactive power are calculated from (9), and the algorithm is terminated.

4. Performance evaluation

The performance of the proposed method is evaluated in this section using extensive simulations conducted on the IEEE 39-bus test system [35]. First, a general performance evaluation is presented to show the ability of the method to identify the size and location of LoG events considering RESs with different control settings. The outages of both SGs and RESs under different loading conditions are studied. Then, the accuracy of the estimated nodal current injections representing non-monitored RESs during different LoG events is examined. The control settings and locations of RESs summarized in Table 1 are considered in Subsections 4.1, 4.2, 4.3, and 4.4. Next, a comparison study is conducted between the proposed and the existing methods from different viewpoints. The method's sensitivity to measurement, parameter, and topology errors is also investigated. Then, the minimum LoG size the method can detect is scrutinized. Twelve PMUs are placed at buses 3, 5, 8, 11, 14, 16, 19, 23, 25, 27, 29, and 39 [36]. The impact of different numbers and locations of PMUs on the LoG size estimation is also scrutinized in Subsection 4.4. Finally, the impact of the RESs penetration is assessed by maintaining the total active power generation of the system while changing the share, location, and control settings of RESs.

Extensive time-domain simulations are conducted using DIgSILENT PowerFactory. An anti-aliasing Butterworth filter with a cut-off frequency of 400 Hz is used to filter the recorded current and voltage waveforms, which are sampled at a frequency of 2 kHz. Then, the discrete Fourier transform is applied to estimate the phasors of these waveforms. The LoG size is reported as the average of its estimation over one power-frequency cycle. This calculation is performed after a full data window length from the LoG onset to account for the transient response of the phasor estimation process, over which the estimated phasor is not accurate [8].

4.1. General evaluation of the proposed method

As listed in Table 1, a set of 20 RESs with different settings are connected at random locations in the IEEE 39-bus test system. To demonstrate the performance of the proposed method, two arbitrary outages are examined. The first LoG event is the outage of the SGs connected to bus 33, resulting in the loss of 320 MW active power. The second LoG event is the outage of the RES connected to bus 24, with 135 MW active power injection prior to the event. Fig. 3 and Fig. 4 show the *SoSR* of all candidate LoG locations for the SGs outage and RES outage, respectively, for up to 200 ms following the LoG event.

Table 1
Settings and locations of RESs.

Location (Bus No.)	Control Settings
1,5,7,9,12, 14,15,17,24,26	Sn= 150 MVA P_{ref}= 0.9 pu, Q_{ref}= 0.1 pu
3,4,8,11,13,16,18,21,27,28	Sn= 200 MVA P_{ref}= 0.85 pu, Q_{ref}= 0.15 pu

In both cases, the *SoSR* of the tripped generation is the least *SoSR* amongst the *SoSRs* calculated for all candidate LoG locations. This confirms the ability of the proposed method to correctly identify the LoG location regardless of whether it is the outage of SGs or RES. Simulation results show that the *SoSR* index remains valid for identifying the LoG location accurately for up to one second.

Fig. 5 shows the estimated LoG sizes, i.e., changes in active and reactive power injections, over time for LoG events at the foregoing locations. In this figure, the actual values of ΔP and ΔQ are indicated by dotted lines. It is evident that accurate LoG size estimations can be achieved after one power-frequency cycle from the LoG onset.

Existing methods do not account for the presence of RESs in the system. As expected, these methods become less reliable as the share of RESs increases. The proposed method incorporates the RESs into the formulation by directly adding the superimposed currents of monitored RESs and estimating those of the non-monitored RESs. To show this, the total vector errors (TVEs) between the estimated superimposed currents of the non-monitored RESs and their corresponding true values are reported in percentage in Table 2. The TVE index is used to quantify the error between two phasors, which combines the amplitude and phase-angle errors between them [37]. While existing methods disregard the presence of RESs, the maximum TVE for the estimated superimposed currents of RESs with the proposed method is less than 15%. This means the proposed method incorporates the contribution of RESs into the formulation with an accuracy of more than 85%. As will be shown, estimating the contributions of RESs is quite advantageous for the main objectives of the method, i.e., accurate LoG location and size estimation.

To test the method under different loading conditions, light-load and heavy-load scenarios are created by applying a uniform 50% increase/decrease to all loads/generations in the base case scenario. Table 3 and Table 4 summarize the percentage errors of the size estimations for LoG events at 30 ms after the LoG onset. It can be seen that the size of the LoG event is accurately estimated in all cases, with errors up to 1.52% and 1.63% for SG and RES outages, respectively. This indicates that the proposed method can accurately estimate the size of LoG events regardless of the loading condition. The estimated LoG size is more accurate if it is performed in the first few cycles following the LoG event instant.

As per the extensive simulations conducted, the average number of iterations taken by the proposed method is 4.5. For the IEEE 39-bus test system with 10 SGs and 20 RESs, the overall computation time amounts to less than 20 ms on a 2.8 GHz processor with 8 GB of RAM. It should be pointed out that the calculations of *SoSRs* are completely independent of each other. Therefore, in a system with very large numbers of candidate LoG locations, the computational burden can be reduced to the calculation of one *SoSR* if the calculations are carried out on parallel processors. On the other hand, the effective technique proposed by the authors in [28] can also be used to limit the calculations to the disturbed area only.

4.2. Comparison with existing methods

The proposed method's performance is compared with that of other methods in this subsection. The superiority of the proposed method can be seen from Table 5, which is not a surprise as the existing methods do not account for the presence of RESs [26,27]. Furthermore, the majority of existing methods demand full network observability, which requires the reception of a specific set of PMU data to make a decision. The

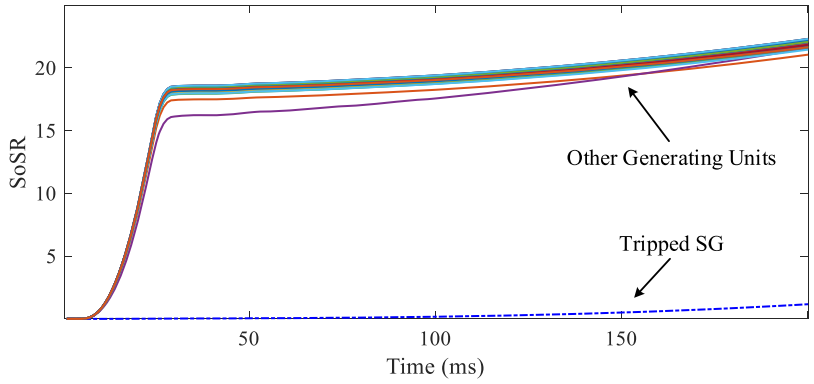

Fig. 3. *SoSR* of all candidate LoG locations after the SG outage at bus 33.

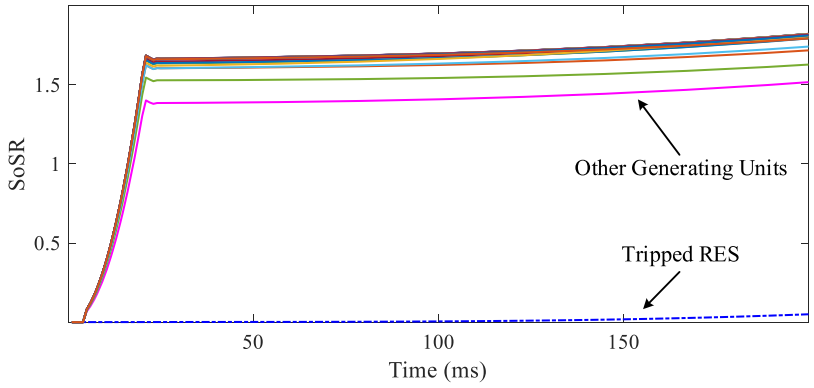

Fig. 4. *SoSR* of all candidate LoG locations after the RES outage at bus 24.

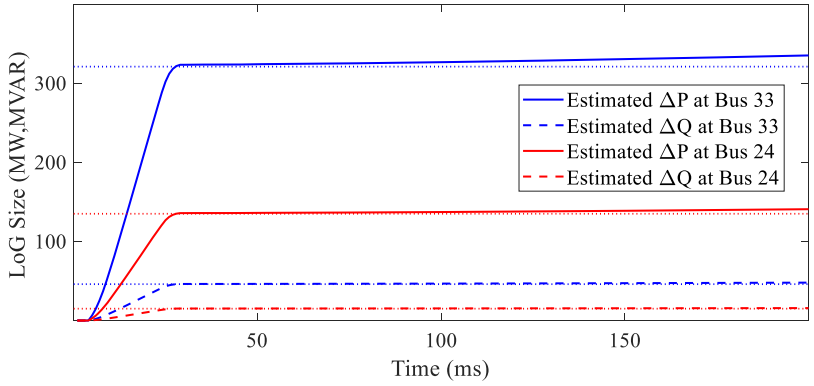

Fig. 5. LoG size estimation following outages at buses 24 and 33.

Table 2
TVE in (%) of the estimated superimposed current of RESs.

LoG Event	RESs Location (Bus No.)									
	4	7	12	13	15	17	18	21	26	28
LoG1*	14.2	14.6	14.1	14.9	13.0	13.9	14	13.05	14.8	14.37
LoG2**	12.5	12.1	12.7	12.6	14.0	14.1	14.4	14.4	12.9	12.3

* Outage of SGs connected to bus 33.
** Outage of RES connected to bus 24.

methods that divide the power system into several zones and need extensive offline studies impose a high computational burden. According to Table 5, the method presented in [25] has a better performance than the other LoG size/location estimation methods. Therefore, the performance comparison is carried out only between the proposed method and the method of [25].

As explained, the true LoG location is determined based on the minimum *SoSR* obtained. Ignoring the presence of RESs by the existing methods introduces inaccuracies into the system model, which results in a higher value for the *SoSR* of the tripped generation. Simulations show

Table 3
LoG size estimation errors in (%) for SG outages.

Scenario	LoG Location (Bus No.)									
	30	31	32	33	34	35	36	37	38	39
Base-case	0.64	1.52	0.15	1.4	0.06	0.08	0.25	0.01	0.84	0.56
Light-load	0.32	0.11	0.08	1.51	0.07	0.07	0.28	0.01	0.26	0.17
Heavy-load	0.72	1.52	0.14	1.28	0.04	0.16	0.20	0.02	1.12	0.92

Table 4
Log size estimation errors in (%) for RES outages.

Scenario	LoG Location (Bus No.)									
	4	7	12	13	15	17	18	21	26	28
Base-case	0.07	0.68	1.01	1.63	0.01	0.25	0.19	1.50	0.15	0.66
Light-load	0.09	0.63	0.97	1.62	0.02	0.18	0.10	1.61	0.29	0.62
Heavy-load	0.09	0.68	1.03	1.60	0.01	0.35	0.30	1.39	0.03	0.68

Table 5
Comparison of the proposed method with existing methods.

Reference	[20]	[21]	[23]	[24]	[25]	Prop.
Consider impact of RESs?	No	No	No	No	No	Yes
Need offline studies?	Yes	Yes	No	No	No	No
Specific sensor locations?	Yes	Yes	Yes	Yes	No	No
Tolerate Sensor Losses?	No	Yes	No	Yes	Yes	Yes
Estimate both size and location?	No	No	No	Yes	Yes	Yes
Computational burden?	High	High	Low	High	Low	Low

Table 6
General performance of the proposed method.

LoG event	Size Estimation Error (%)			
	Proposed method		Method in [25]	
	Ave.	Max.	Ave.	Max.
LoG of SGs	0.55	1.52	7.98	16.81
LoG of RESs	0.33	1.63	N/A	N/A

Table 7
Sensitivity to measurement errors.

Results	Variation Range for Measurement Errors (%)				
	±1	±2	±3	±4	±5
Ave. Error (%)	0.46	0.53	0.64	0.71	0.79
Max. Error (%)	1.91	2.38	3.20	4.18	4.90

Table 8
Sensitivity to generator/line parameter errors.

Variation Range of Errors (%)		±1	±2	±3	±4	±5
Error in Gen. Parameters	Ave. Error (%)	0.45	0.45	0.46	0.46	0.47
	Max. Error (%)	1.66	1.70	1.75	1.78	1.83
Error in Line Parameters	Ave. Error (%)	0.45	0.57	0.68	0.84	0.99
	Max. Error (%)	3.28	6.71	7.36	8.73	13.68

that locating the LoG event by the method of [25] fails in up to 10% of cases with a high penetration of RESs, while the proposed method is 100% successful. This is illustrated by the *SoSR*s obtained for an arbitrary LoG event at bus 36 with the method of [25] and the proposed method. As shown in Fig. 6, the *SoSR* for the true LoG location is noticeably reduced by the proposed method. As shown in Table 6, considering the impact of the RESs penetration can also improve the accuracy of LoG size estimation by up to 15%. Furthermore, in contrast to the existing method, the proposed method is able to locate and estimate the size of tripped RESs, which is quite important in modern power systems with high penetration of renewables.

4.3. Sensitivity to measurement, parameter, and topology errors

In this subsection, the proposed method's performance is assessed for a wide range of errors in measurements, generator/transmission line parameters, and topology. The sources of errors considered in measurements are measurement noises, instrument equipment errors, and phasor estimation errors [38]. The errors are assumed to have normal distributions with mean zero. Table 7 reports the average and maximum LoG size estimation errors for up to ±5% measurement errors. The variation ranges of errors are reported regarding the three-sigma criterion [28]. In this study, each simulated case is repeated 500 times. With up to 5% errors in the measurements, the size estimation remains highly accurate, with a mean and maximum error of 0.79% and 4.9%, respectively. Besides, the LoG event is successfully located in all

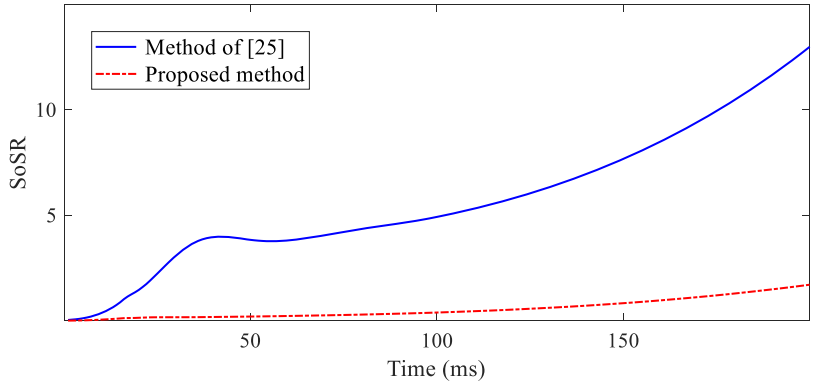

Fig. 6. *SoSR* of the tripped generation at bus 36 using different methods.

simulated cases. The results obtained with errors in generator and transmission line parameters are summarized in Table 8. Again, each simulated case is repeated 500 times. It can be concluded that the method is quite robust to line and generator parameters errors, given the success in LoG location for all cases. As expected, the size estimation accuracy decreases as the parameter errors increase.

The proposed method can function with any given topology so long as the control center constantly updates the network topology for the correct functioning of the EMS applications [39]. This is to ensure possible changes in the system topology will not adversely impact the method's performance. Nevertheless, if changes in the system topology remain unreported to the control center, this might lower the method's success rate. In what follows, we have evaluated the method's performance against topology errors. Table 9 summarizes simulation results and demonstrates the impact of topology errors on LoG location and size estimations following LoG events at different locations in the system. It can be seen that the average success rate for the studied cases is 96.6%, while the average size estimation error is around 6.54%. As expected, the topology error (which may, for example, arises due to misreading of the status of an element) reduces the success rate of the LoG location. In this sense, the proposed method is vulnerable to unreliable inputs similar to any other wide-area monitoring, protection, and control methods.

System operators can hugely benefit from reliable identification of large LoG events [26,27]. Therefore, it is also reasonable to define a threshold for the minimum LoG size to be detected by the method. A sensitivity analysis is performed here to evaluate the minimum detectable LoG size at 20 generation buses by considering random measurement errors of 1% and 5% magnitudes, based on the three sigma criterion [28]. The size of the LoG event is reduced in 2% steps at each certain location, and each simulation case is repeated 500 times to account for the probabilistic nature of errors. The minimum detectable LoG sizes that are successfully located by the proposed method are reported in Fig. 7.

The proposed method takes advantage of the redundancy of PMU data and the least-squares method to minimize the overall effect of errors. Indeed, the availability of more input measurements improves the method's accuracy [40]. Larger numbers of PMUs will help reduce the minimum detectable LoG size. The minimum detectable LoG sizes are reported in Fig. 8 for two arbitrary buses 26 and 34. These are obtained for different numbers of PMUs, while measurements are assumed to have up to 1% errors.

4.4. Observability and PMU coverage

The proposed method is able to locate and accurately estimate the size of LoG events using a limited number of PMUs. The method does not rely upon a fixed set of PMUs, which means its performance will not be necessarily impacted if some PMU data are lost. Nonetheless, the more the number of input measurements, the more accurate the method becomes [40]. To show this, the proposed method is tested with a different number of PMUs. For each scenario, 100 different PMU placements are considered such that each placement leads to a solvable system of equations with a unique solution. As summarized in Table 10, the LoG size is accurately estimated in all scenarios. This confirms that the PMU placement does not remarkably affect the method's performance.

Table 9
LoG location and size estimation sensitivity to topology errors.

Transmission Line/ Transformer Index	Success Rate of LoG Location (%)		Ave. Size Estimation Error (%)	
	Not Considered while in Service	Considered while not in Service	Not Considered while in Service	Considered while not in Service
5–8	93.01	99.01	9.46	2.83
11–12	96.52	99.21	2.21	4.96
17–18	93.01	98.65	12.89	6.86

4.5. Sensitivity to the number and locations of RESs

The proposed method can easily be applied to power systems with different locations and penetration levels of RESs. To demonstrate this, four different penetration levels are considered. The penetration level of RESs in the first column of Table 11 is obtained by modifying the control settings reported in Table 1. In doing so, the nominal powers of RESs are changed to obtain different injections of active power. For each penetration level, the simulation is repeated 20 times with different numbers and locations of RESs. The results presented in Table 11 show that the proposed method provides acceptable LoG size estimation regardless of the penetration level, number, and locations of RESs. Increased penetration of RESs adversely affects the existing methods in estimating the LoG size, while this is not the case with the proposed method.

4.6. Practical application: under-frequency load shedding

The proposed method could be incorporated into a centralized UFLS scheme as it can promptly identify the location and size of LoG events. Timely identification of LoG events is advantageous to preserving the power system's stability. This enables the disconnection of loads from the vicinity of the LoG location as early as possible. Here, we compare the performance of the conventional UFLS scheme with that of a centralized UFLS scheme by taking advantage of the proposed method. As an example, the LoG event is considered to be the outage of 1200 MW active power. In this example, the RES penetration level is 40%, while the total system inertia is 2.7 s. The conventional UFLS scheme is set to shed up to 30% of the total load through 4 steps of 7.5% each. Load shedding is initiated at 49.5 Hz, and the frequency thresholds for each step are set 0.3 Hz apart. Fig. 9 illustrates the frequency response of the center of inertia of the system following the LoG event. Thanks to the LoG size estimated, the centralized UFLS scheme can trip a total amount of load equal to the amount of generation lost, i.e., β=1 pu. This is accomplished by shedding loads from the vicinity of the LoG event, i.e., buses 3, 4, 7, 8, 15, 20, and 39. It can be seen that the frequency nadir is enhanced by 0.28 Hz compared to the conventional UFLS. By setting β=0.75 pu, the proposed scheme sheds the same amount of load as is shed by the conventional scheme. This increases the frequency nadir by 0.2 Hz compared to the latter. These results demonstrate the improvement in the frequency response achieved by the centralized UFLS scheme. Moreover, load shedding from the vicinity of the LoG event could be highly advantageous against combinational voltage and frequency instabilities [30].

5. Conclusion

This paper proposes a method for estimating the size and location of loss of generation (LoG) events in power systems with high penetration of renewable energy sources (RESs). The method uses the superimposed circuit methodology to account for the contribution of RESs using available PMU measurements. An overdetermined system of linear equations is obtained by manipulating the bus impedance matrix with reference to active and reactive power setpoints of RESs, and available PMU data. The solvability concerns of the system of equations are hugely reduced by estimating the contribution of non-monitored RESs. The solution of this system provides the superimposed current injection of the tripped generation. The proposed method relies merely on rigorous KVL and KCL equations. Thus, it is faster than existing methods based on frequency measurements and more accurate than those requiring the knowledge of system inertia.

The presence of RESs is not considered by existing methods, which introduces significant errors if the penetration level is high. The proposed method is able to locate and estimate the size of LoG events with

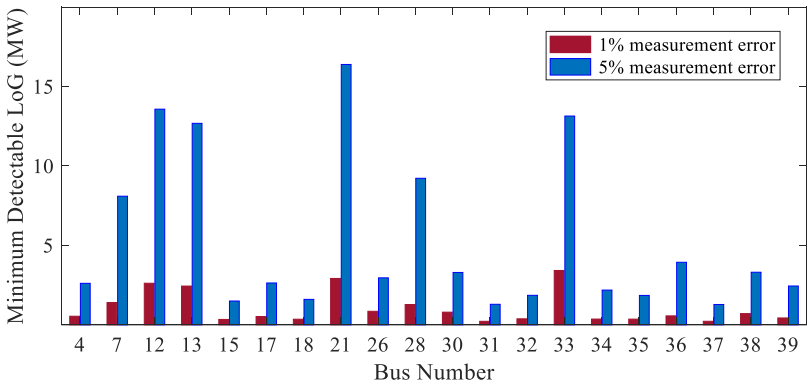

Fig. 7. Impact of measurement errors on the minimum detectable LoG size.

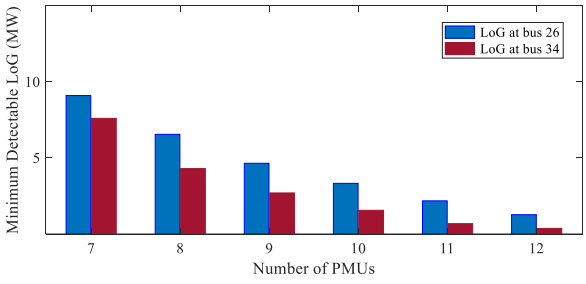

Fig. 8. Impact of the number of PMUs on the minimum detectable LoG size.

Table 10
Sensitivity to the number of PMUs.

Results	Number of PMUs				
	12	11	10	9	8
Ave. Error (%)	0.60	0.66	0.70	0.81	0.80

Table 11
Sensitivity to settings, number, and locations of RESs.

Share of RESs from Generation	Number of RESs	24	20	16	12
40%	Ave. Size Estimation Error (%)	0.38	0.38	0.40	0.40
50%		0.39	0.40	0.41	0.44
60%		0.41	0.45	0.43	0.52
70%		0.42	0.49	0.45	0.56

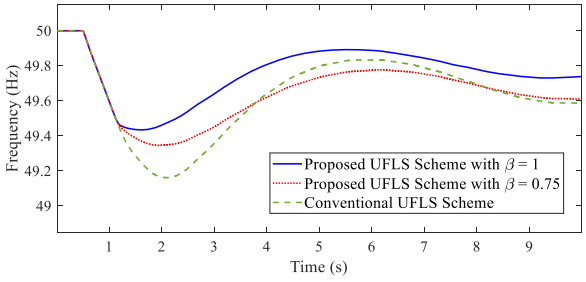

Fig. 9. Frequency response following UFLS based on different schemes.

high accuracy regardless of whether the tripped generation is a synchronous generator or an RES. More importantly, there are no rigid constraints on the number and location of PMUs to obtain reliable estimations. Hence, if any PMU data is temporarily lost, the accuracy of the results is not noticeably affected. The proposed method demonstrates robustness against measurement and parameter errors. It is also shown that different numbers, locations, and penetration levels of RESs do not have a meaningful impact on the performance of the proposed method.

CRediT authorship contribution statement

Jesús Sánchez Cortés: Conceptualization, Methodology, Writing – original draft. **Mohammad Rezaei Jegarluei:** Software, Validation, Data curation. **Petros Aristidou:** Resources, Investigation, Validation. **Kang Li:** Resources, Writing – review & editing. **Sadegh Azizi:** Writing – review & editing, Formal analysis, Validation, Supervision.

Declaration of Competing Interest

The authors declare that they have no known competing financial interests or personal relationships that could have appeared to influence the work reported in this paper.

Data availability

No data was used for the research described in the article.

References

[1] D. Zografos, M. Ghandhari, Power system inertia estimation by approaching load power change after a disturbance, 2017 IEEE Power & Energy Soc. General Meeting (2017) 1–5.
[2] National Grid ESO, The Enhanced Frequency Control Capability (EFCC) Project Closing Down Report, 2019 [Online]. Available: https://www.nationalgrideso.com/future-energy/projects/enhanced-frequency-control-capability-efcc.
[3] P. Tielens, D.V. Hertem, The relevance of inertia in power systems, Renew. Sustain. Energy Rev. 55 (2016) 999–1009, https://doi.org/10.1016/j.rser.2015.11.016 [Online] Available:.
[4] MIGRATE, Development and tests of new protection solutions when reaching 100% PE penetration. EU H2020 MIGRATE Project, Deliverable 4.3, Tech. Rep, Dec. 2018.
[5] P.S. Kundur. Power System Stability and Control, McGraw-Hill, New York, NY, USA, 1994.
[6] ENTSO-E, Future System Inertia, Tech. Rep, Belgium, 2018. Feb.
[7] Y. Zhang, et al., Wide-area frequency monitoring network (FNET) architecture and applications, IEEE Trans. Smart Grid 1 (2) (Sep. 2010) 159–167.
[8] P.M. Anderson, Power System Protection, IEEE Press, New York, 1999.
[9] V. Terzija, Adaptive underfrequency load shedding based on the magnitude of the disturbance estimation, IEEE Trans. Power Syst. 21 (3) (Aug. 2006) 1260–1266.
[10] M. Sun, et al., Underfrequency load shedding using locally estimated rocof of the center of inertia, IEEE Trans. Power Syst 36 (5) (Sep. 2021) 4212–4222.
[11] J. Dong, et al., Analysis of power system disturbances based on wide-area frequency measurements, 2007 IEEE Power Eng. Soc. General Meeting (2007) 1–8.
[12] A. Bykhovsky, J.H. Chow, Power system disturbance identification from recorded dynamic data at the Northfield substation, Int. J. Electric. Power & Energy Syst. 25no (10) (2003) 787–795, https://doi.org/10.1016/S0142-0615(03)00045-0 [Online] Available:.
[13] J.N. Bank, et al., Generator trip identification using wide-area measurements and historical data analysis, in: 2006 IEEE PES Power Systems Conference and Exposition, 2006, pp. 1677–1681.

[14] W. Li, J. Tang, J. Ma, Y. Liu, Online detection of start time and location for hypocenter in North America power grid, IEEE Trans. Smart Grid 1 (3) (Dec. 2010) 253–260.
[15] T. Xia, et al., Wide-area frequency based event location estimation, 2007 IEEE Power Eng. Soc. General Meeting (2007) 1–7.
[16] G. Zheng, Y. Liu, G. Radman, Wide area frequency based generation trip event location estimation, 2012 IEEE Power and Energy Soc. General Meeting (2012) 1–6.
[17] W.-T. Li, et al., Location identification of power line outages using PMU measurements with bad data, IEEE Trans. Power Syst. 31 (5) (Sep. 2016) 3624–3635.
[18] G. Frigo, A. Derviškadić, Y. Zuo, M. Paolone, PMU-based rocof measurements: uncertainty limits and metrological significance in power system applications, IEEE Trans. Instrum. and Meas. 68 (10) (Oct. 2019) 3810–3822.
[19] U. Rudez, R. Mihalic, Analysis of underfrequency load shedding using a frequency gradient, IEEE Trans. Power Del. 26 (2) (Apr. 2011) 565–575.
[20] H. Zhang, F. Shi, Y. Liu, V. Terzija, Adaptive online disturbance location considering anisotropy of frequency propagation speeds, IEEE Trans. Power Syst. 31 (2) (Mar. 2016) 931–941.
[21] D.-I. Kim, A. White, Y. Shin, PMU-based event localization technique for wide-area power system, IEEE Trans. Power Syst. 33 (6) (Nov. 2018) 5875–5883.
[22] S.M. Rovnyak, K. Mei, Dynamic event detection and location using wide area phasor measurements, Eur. Trans. Elect. Power (2010).
[23] R. Azizipanah-Abarghooee, M. Malekpour, M. Paolone, V. Terzija, A new approach to the online estimation of the loss of generation size in power systems, IEEE Trans. Power Syst. 34 (3) (May 2019) 2103–2113.
[24] N. Shams, P. Wall, V. Terzija, Active power imbalance detection, size and location estimation using limited PMU measurements, IEEE Trans. Power Syst. 34 (2) (Mar. 2019) 1362–1372.
[25] S. Azizi, et al., Wide-area identification of the size and location of loss of generation events by sparse PMUs, IEEE Trans. Power Del. 36 (4) (Aug. 2021) 2397–2407.
[26] M.R. Jegarluei, J.S. Cortés, S. Azizi, V. Terzija, Wide-area event identification in power systems: a review of the state-of-the-art, in: 2022 IEEE International Conference on Smart Grid Synchronized Measurements and Analytics (SGSMA), Split, Croatia, 2022, pp. 1–7.
[27] S. Azizi, M. Rezaei Jegarluei, J. Sánchez Cortés, V. Terzija, State of the art, challenges and prospects of wide-area event identification on transmission systems, Int. J. Electric. Power & Energy Syst. 148 (2023).
[28] S. Azizi, M. Sanaye-Pasand, From available synchrophasor data to short-circuit fault identity: formulation and feasibility analysis, *IEEE Trans. Power Syst* 32 (3) (May 2017) 2062–2071.
[29] K. Jia, et al., Influence of inverter interfaced renewable energy generators on directional relay and an improved scheme, IEEE Trans. Power Electron. 34 (12) (Dec. 2019) 11843–11855.
[30] M. Abedini, M. Sanaye-Pasand, S. Azizi, Adaptive load shedding scheme to preserve the power system stability following large disturbances, IET Gener. Transm. Distrib. 8 (2014) 2124–2133, https://doi.org/10.1049/iet-gtd.2013.0937 [Online] Available:.
[31] A.S. Dobakhshari, S. Azizi, M. Paolone, V. Terzija, Ultra fast linear state estimation utilizing SCADA measurements, IEEE Trans. Power Syst. 34 (4) (2019) 2622–2631.
[32] C.D. Meyer, Matrix Analysis and Applied Linear Algebra, SIAM, Philadelphia, PA, USA, 2001.
[33] National Grid ESO, *The Grid code, Issue 6, Revision 12*", Mar. 2022. Great Britain [Online] Available: https://www.nationalgrideso.com/industry-information/codes/grid-code/code-documents.
[34] Tennet TSO GmbH, Grid Code—High and Extra High Voltage, 2017 [Online] Available: https://www.tennet.eu/nl/elektriciteitsmarkt/regels-en-procedures/europese-codes/.
[35] R.D. Zimmerman, C.E. Murillo-Sanchez, D. Gan, MATPOWER, a MATLAB Power System Simulation Package, 2007 ver. 3.2[Online]. Available, http://www.pserc.cornell.edu/matpower/.
[36] S. Azizi, A.S. Dobakhshari, S.A.N. Sarmadi, A.M. Ranjbar, Optimal PMU placement by an equivalent linear formulation for exhaustive search, IEEE Trans. Smart Grid 3 (1) (2012) 174–182.
[37] IEEE Standard for Synchrophasor Measurements For Power Systems, IEEE Std, 2011. C37.118.1-2011.
[38] S. Sarri, M. Pignati, P. Romano, L. Zanni, M. Paolone, A hardware-in-the-loop test platform for the performance assessment of a PMU-based real-time state estimator for active distribution networks, in: Proc. IEEE PowerTech, Jun. 2015, pp. 1–6. Eindhoven, The Netherlands.
[39] A. Abur, A.G. Exposito. Power System State Estimation: Theory and Implementation, Marcel Dekker, Inc., 2004.
[40] F.C. Schweppe, J. Wildes, Power system static-state estimation, part I: exact model, IEEE Trans. Power Apparatus and Syst. PAS-89 (1) (Jan. 1970) 120–125.